Bering Strait Ocean Heat Transport Drives Decadal Arctic Variability in a High-Resolution Climate Model

Yuchen Li[1], Wilbert Weijer[2], Prajvala Kurtakoti[3], Milena Veneziani[2], and Ping Chang[4]

[1]Stanford University
[2]Los Alamos National Laboratory (DOE)
[3]Los Alamos National Laboratory
[4]TAMU

March 15, 2024

Abstract

We investigate the role of ocean heat transport (OHT) in driving the decadal variability of the Arctic climate by analyzing the pre-industrial control simulation of a high-resolution climate model. While the OHT variability at 65@N is greater in the Atlantic, we find that the decadal variability of Arctic-wide surface temperature and sea ice area is much better correlated with Bering Strait OHT than Atlantic OHT. In particular, decadal Bering Strait OHT variability causes significant changes in local sea ice cover and air-sea heat fluxes, which are amplified by shortwave feedbacks. These heat flux anomalies are regionally balanced by longwave radiation at the top of the atmosphere, without compensation by atmospheric heat transport (Bjerknes compensation). The sensitivity of the Arctic to changes in OHT may thus rely on an accurate representation of the heat transport through the Bering Strait, which is difficult to resolve in coarse-resolution ocean models.

Bering Strait Ocean Heat Transport Drives Decadal Arctic Variability in a High-Resolution Climate Model

Yuchen Li[1,2*], Wilbert Weijer[2,3], Prajvala Kurtakoti[4,2], Milena Veneziani[2], Ping Chang[5]

[1]Stanford University, Stanford, CA, USA
[2]Los Alamos National Laboratory, Los Alamos, NM, USA
[3]International Arctic Research Center, University of Alaska Fairbanks, Fairbanks, AK, USA
[4]Johns Hopkins University, Baltimore, MD, USA
[5]Texas A&M University, College Station, TX, USA

Key Points:

- Ocean heat transport variability through the Bering Strait has an outsized effect on Arctic sea ice cover and surface temperature
- Atlantic ocean heat transport anomalies into the Arctic are compensated by atmospheric heat transport anomalies on decadal timescales

*450 Jane Stanford Way Stanford, CA 94305–2004

Corresponding author: Yuchen Li, `yucli@stanford.edu`

Abstract

We investigate the role of ocean heat transport (OHT) in driving the decadal variability of the Arctic climate by analyzing the pre-industrial control simulation of a high-resolution climate model. While the OHT variability at 65°N is greater in the Atlantic, we find that the decadal variability of Arctic-wide surface temperature and sea ice area is much better correlated with Bering Strait OHT than Atlantic OHT. In particular, decadal Bering Strait OHT variability causes significant changes in local sea ice cover and air-sea heat fluxes, which are amplified by shortwave feedbacks. These heat flux anomalies are regionally balanced by longwave radiation at the top of the atmosphere, without compensation by atmospheric heat transport (Bjerknes compensation). The sensitivity of the Arctic to changes in OHT may thus rely on an accurate representation of the heat transport through the Bering Strait, which is difficult to resolve in coarse-resolution ocean models.

Plain Language Summary

We studied how ocean heat transport (OHT) affects decade-timescale variability in the Arctic climate using a high-resolution climate model. Specifically, we compared the impacts of heat entering the Arctic Ocean through the Nordic Seas from the Atlantic and through the Bering Strait from the Pacific. Though more heat is transported from the Atlantic, Arctic surface temperature and sea ice respond more strongly to changes in OHT through the Bering Strait. Unlike Atlantic OHT, changes in Bering Strait OHT impact local air temperatures directly, without compensating changes in atmospheric heat transport. Proper representation of the Arctic's sensitivity to future increased OHT may thus rely on correctly representing OHT through Bering Strait, which is challenging in coarse-resolution ocean models.

1 Introduction

The Arctic is warming faster than the rest of the world (Rantanen et al., 2022; Chylek et al., 2022). This amplification of Arctic climate change is caused by a coupling between local feedbacks and increased poleward heat transport from lower latitudes (Hwang et al., 2011; Nummelin et al., 2017; Previdi et al., 2021). However, the mechanisms of this coupling are complex and still poorly understood.

Decadal to multidecadal timescale variability in the Arctic—manifested by changes in sea ice extent, surface temperatures, etc.—has been previously shown to be closely related to ocean heat transport (Zhang, 2015; Jungclaus & Koenigk, 2010). Further, it has been suggested that variability in *total* heat transport into the Arctic is reduced by a phenomenon known as Bjerknes Compensation (BC), whereby anomalies in meridional ocean heat transport (OHT) tend to induce roughly equal and opposite anomalies in meridional atmospheric heat transport (AHT). Bjerknes (1964) proposed that this result follows from energy conservation on timescales where the top-of-atmosphere (TOA) fluxes and ocean heat content remain approximately constant. A recent study (Y. Liu et al., 2020) indeed found evidence of decadal-timescale BC in several reanalysis datasets and confirmed the importance of surface heat fluxes in communicating OHT variability to the atmosphere. However, as they note, the exact causal relationships of decadal-timescale heat transport variability are very difficult to parse out in such short observational time series.

Models have thus been indispensable to the study of BC due to the need for sufficiently long time series. In coupled global climate models, BC is typically strongest at the high northern latitudes (Shaffrey & Sutton, 2006; Swaluw et al., 2007; Outten & Esau, 2017; Jungclaus & Koenigk, 2010), due to the presence of strong regional climate feedbacks in the marginal ice zone (Z. Liu et al., 2016; Kurtakoti et al., 2023). Specifically, Swaluw et al. (2007) and Outten and Esau (2017) argue that BC in high northern latitudes is due to the modulation of sea ice by decadal Atlantic OHT variability. The canonical mechanism is illustrated as follows: positive OHT anomalies melt back sea ice, enhancing heat loss from the previously ice-covered ocean. The anomalous heat flux into the atmosphere may be amplified by local radiative feedbacks such as the ice-albedo feedback, causing local atmospheric warming. This warming then reduces the meridional temperature gradient and thus baroclinity, reducing the northward heat transport by atmospheric eddies.

This canonical perspective does not take into account significant longitudinal variations in the Earth's geography and climate mean state. In particular, OHT from the sub-Arctic to the Arctic Ocean takes place primarily through two main gateways: flow across the Greenland-Scotland Ridge connects the Arctic Ocean to the subpolar North Atlantic Ocean, while flow through the Bering Strait connects the Arctic to the subpolar North Pacific. OHT through the Atlantic sector is an order of magnitude larger than that through the Bering Strait, both in mean value and in amplitude of variability. Consequently, most studies on the connection between decadal Arctic variability and Bjerknes Compensation have focused mainly on Atlantic OHT variability. An exception is the study by Li et al. (2018), who analyzed three Earth system models (ESM) and demonstrated that OHT through both gateways has an important impact on Arctic climate. In fact, they argue that OHT through Bering Strait is more efficient in causing low-frequency variability of Arctic sea ice than OHT through the Atlantic sector. A strong sensitivity of Arctic sea ice on Bering Strait throughflow has also been found in observations (Woodgate et al., 2012; MacKinnon et al., 2021).

This raises the question: how does the atmosphere respond to OHT variability through the different gateways given the differences in sea ice sensitivity, and what are the consequences for the atmosphere's ability to compensate for this OHT variability?

This question is important for several reasons. First, observations over the past few decades (Woodgate, 2018; Tsubouchi et al., 2021) as well as model projections of future climate change (Shu et al., 2022) show a robust increase of northward OHT going into the Arctic from both the subpolar North Atlantic and North Pacific Oceans. The extent to which AHT will compensate these changes is therefore of primary concern for constraining uncertainty in Arctic climate change. Second, the current generation of climate models typically have a spatial resolution of $\sim 1^\circ$ in their standard configuration ocean models. Such low resolution leaves narrow channels like the Bering Strait significantly underresolved (Chang et al., in review), while poorly resolved bathymetry also appears to weaken OHT across the Greenland-Scotland Ridge (Heuzé & Årthun, 2019). Consequently, OHT in standard resolution climate models may be significantly biased, and their results should be treated with caution.

Recently, an unprecedented multi-century simulation of a high-resolution global climate model was performed (Chang et al., 2020), which at the time of analysis was the longest pre-industrial control simulation run at high resolution (see Data and Methods). In this paper we use this unique data set to investigate the Arctic atmospheric response to OHT variability through the primary oceanic gateways. We find that Bering Strait OHT plays an outsized role in driving Arctic climate variability. By decomposing the meridional energy balance, we show that while the AHT partially compensates for anomalies in the zonally-integrated OHT, lateral atmospheric energy fluxes do not compensate for anomalies in OHT through Bering Strait.

2 Data and Methods

We use a portion of the 500-year pre-industrial (PI) control simulation of CESM1.3 (Community Earth System Model version 1.3), configured with nominal horizonal res-

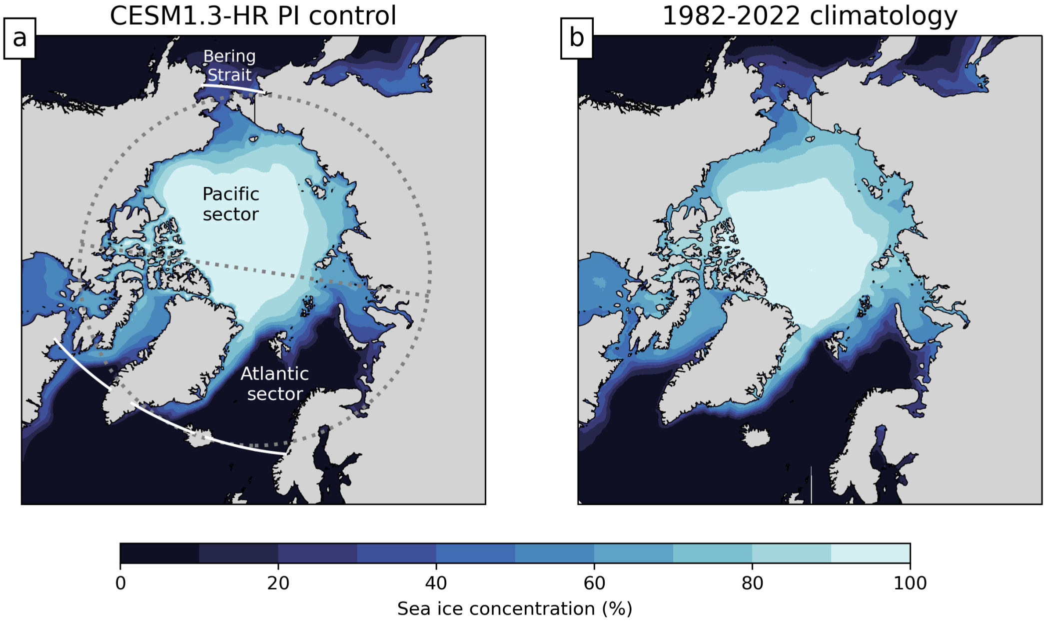

Figure 1. (a) Annual-mean climatology of Arctic sea ice concentration in the PI control simulation analyzed in this study. The dotted grey lines show 65°N and the boundary between the Pacific and Atlantic sectors defined in this paper. The white lines indicate the logical latitudes used for integration. (b) Observed 1982-2022 climatology of annual-mean Arctic sea ice concentration (NOAA OISST v2).

olutions of 0.25°in the atmosphere and land models and 0.1°in the ocean and sea-ice models (Chang et al., 2020). The PI control was forced with greenhouse gas conditions kept constant at the 1850 levels throughout the simulation. We exclude the first 150 years from our analysis due to model drift, so all time series are 350 years long (see Chang et al., 2020, for context). The sea ice climatology of the PI control simulation is shown in Figure 1a and shows good agreement with the observed climatology during the satellite era (Fig. 1b).

We estimate meridional OHT and AHT at 65°N from monthly-averaged fields. We choose 65°N as the boundary of the Arctic, however our results are not sensitive to the choice of latitude. The OHT time series is calculated by integrating the product of meridional velocity (v) and potential temperature (Θ):

$$\mathrm{OHT} = \int_{\varphi_E}^{\varphi_W} \int_{-H}^{0} c_p v \Theta \cos\theta \, \mathrm{d}z \; R_e \mathrm{d}\varphi \tag{1}$$

where we use θ and φ to denote latitude and longitude, respectively. φ_E and φ_W denote the eastern and western boundaries of the basin and H, c_p, z, and R_e denote basin depth, heat capacity of seawater at constant pressure, vertical depth, and the radius of the Earth, respectively. This reconstruction, which ignores contributions by sub-monthly covariance between velocity and temperature, is necessary because the model's online diagnostic OHT output was corrupted for the first 277 years and thus would have significantly shortened the available timespan for our analysis. For ease of computation, we also choose to approximate OHT across 65°N by heat transport across a *logical* latitude line of the model's tripolar grid that tracks 65°N reasonably well. A comparison between our OHT time series, the OHT time series from the model's online diagnostic output across the same logical latitude line (after the period of data corruption), and an estimate of the OHT across the actual 65°N latitude line, shows that our OHT time series is an accurate representation of OHT across 65°N in the Atlantic (Supplementary Information).

The AHT time series is estimated by assuming a negligible atmospheric heat capacity and cumulatively integrating the energy flux divergence (e.g., Shaffrey & Sutton, 2006; Swaluw et al., 2007; Outten et al., 2018). We define AHT at the north pole ($\theta = \pi/2$) to be zero and integrate the zonally-integrated flux divergence southward to find the AHT at each latitude θ:

$$\mathrm{AHT} = \int_{\theta}^{\pi/2} \int_{0}^{2\pi} (F_{\mathrm{sfc}} - F_{\mathrm{TOA}}) R_e^2 \cos\theta' \, \mathrm{d}\varphi \, \mathrm{d}\theta' \tag{2}$$

where F_{TOA} and F_{sfc} are the net downward heat flux at the top-of-atmosphere and surface, respectively. By this formulation, northward AHT is positive.

Since we are concerned with variability on decadal timescales, all monthly time series are annually-averaged, detrended, and then smoothed using a 10-year moving average. Moreover, to account for inflated Pearson's r when regressing smoothed time series, we calculate an effective number of degrees of freedom for significance tests. We follow the formulation given in Jungclaus and Koenigk (2010) to estimate the effective number of samples:

$$n_{\mathrm{eff}} = \frac{n}{1 + 2(\sum_{i=1}^{n} r_i r_i')} \tag{3}$$

where n is the original length of the time series and r_i, r_i' are the autocorrelations of the two time series at lag i. For smoothed time series originally with 341 samples, n_{eff} is on the order of 30-50.

3 Results

3.1 Arctic response to Pacific and Atlantic OHT

The OHT through the Atlantic and Bering Strait (the blue and red lines in Figure 2, respectively) both display decadal to multidecadal variability. OHT anomalies are positively correlated with Arctic-average surface air temperature anomalies and negatively correlated with sea ice area anomalies (Figure 2a,b). Strikingly, Bering Strait OHT (mean = 8.6 TW, standard deviation = 1.4 TW) has a stronger correlation with both surface temperature and sea ice than Atlantic OHT (mean = 342 TW, standard deviation = 10.5 TW), even though it is considerably smaller in magnitude. It is not possible to conclude from correlation alone whether 1) OHT variability is driving these changes in temperature and sea ice, 2) OHT variability is driven by surface temperature changes, or 3) OHT, temperature, and sea ice covary due to another driving mode of variability. In later sections, however, we present evidence indicating that OHT plays the driving role in modulating sea ice and air-sea heat flux, thus communicating ocean heat anomalies to the atmosphere.

At 65°N, anomalies in AHT and Atlantic OHT compensate each other on decadal timescales, with an anticorrelation of $r = -0.61$ (Figure 2c). The compensation is inconsistent over time, with some periods displaying almost perfect compensation, while others show undercompensation (where the magnitude of the AHT anomaly is less than the magnitude of the OHT anomaly) or overcompensation (where the magnitude of the AHT anomaly exceeds the magnitude of the OHT anomaly). Moreover, Bering Strait OHT is not correlated with the AHT. In general, the *total* OHT (not shown here) and AHT anomalies are opposite in sign, indicative of Bjerknes compensation on a decadal timescale.

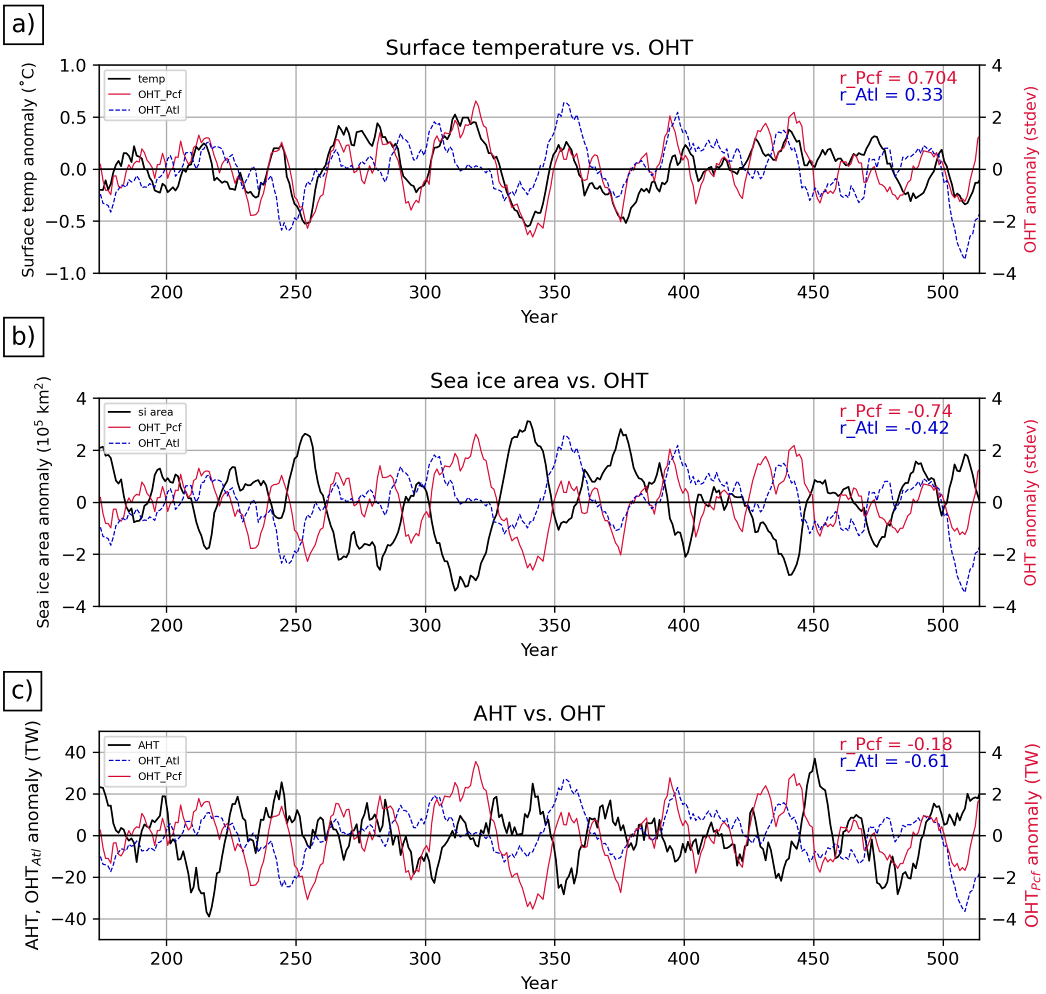

Figure 2. **(a)**: Area-averaged surface air temperature anomaly over the Arctic domain (black) plotted with standardized Bering Strait (red) and Atlantic (blue, dotted) OHT anomalies. **(b)**: same as (a), but sea ice area anomaly (black) is shown instead of temperature. **(c)**: same as (a), but AHT anomaly (black) is shown instead of temperature. The time series are not standardized to emphasize their magnitudes. Note that in (c) the vertical scale for Bering Strait OHT has been magnified by a factor of 10 for better visibility. Pearson's r correlation coefficients are given in the top right.

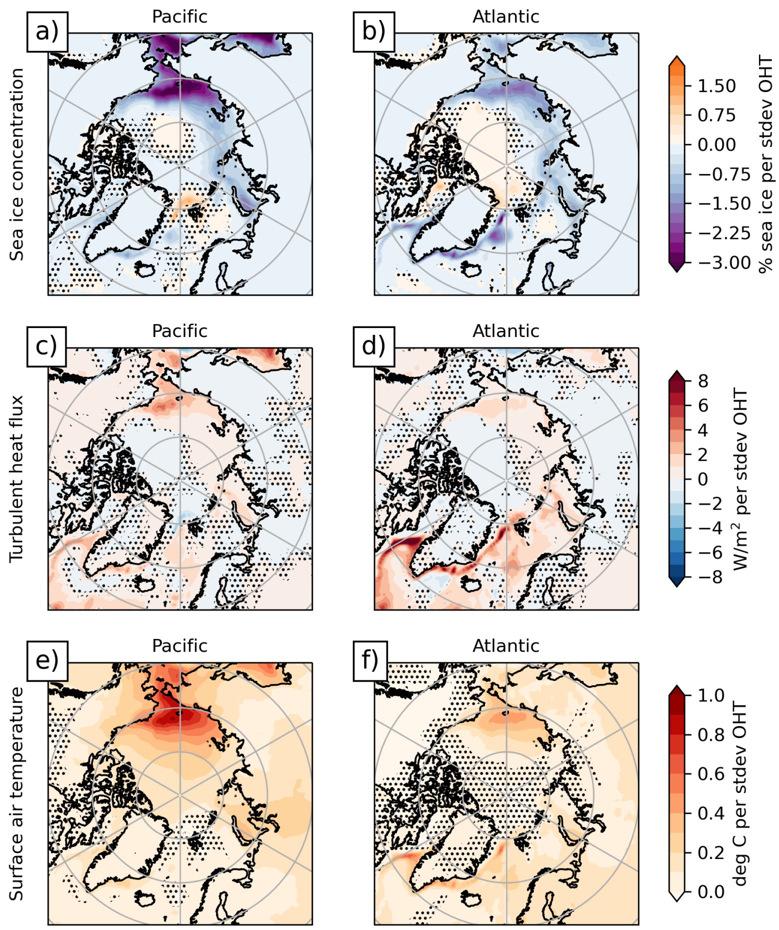

Figure 3. **(a)**: regression of 10-year moving mean sea ice concentration anomalies onto the standardized Bering Strait OHT anomalies at 65°N. Stippling indicates statistical insignificance with respect to a $p = 0.05$ threshold. **(b)**: as in (a), but regressed onto Atlantic OHT. **(c)**: as in (a), but turbulent heat fluxes (defined as sensible plus latent surface heat flux with positive going from ocean to atmosphere). **(d)**: as in (c), but regressed onto Atlantic OHT. **(e):** as in (a), but surface air temperature. **(f):** as in (e), but regressed onto Atlantic OHT.

3.2 Bering Strait OHT Drives Variability in the Pacific Sector

To better understand the atmosphere-ocean interaction that mediates these distinct OHT-AHT relationships, we regress the sea ice anomaly, surface turbulent heat flux (defined as the sum of latent and sensible heat fluxes) anomaly, and surface air temperature anomaly onto the standardized OHT anomaly across 65°N.

Figure 3 shows the linear regressions of anomalous sea ice concentration, turbulent heat flux, and surface temperature onto the OHT anomaly through Bering Strait and the Atlantic separately. During periods of anomalously high OHT, ice is lost in the marginal ice zone and anomalous heat flux is transferred from the newly exposed ocean to the atmosphere. The greatest changes associated with Atlantic OHT variability occur along the East Greenland Current while the greatest changes associated with Bering Strait OHT variability occur in the Chukchi Sea. The greatest changes in surface heat flux are found at the marginal ice zone, similar to what was found in Outten and Esau (2017), Jungclaus and Koenigk (2010), and Kurtakoti et al. (2023). Regression of anomalous sea surface temperatures (SST) onto OHT reveals a spatial pattern similar to the heat flux regression (Figure S1). This positive correlation between SST and heat flux indicates that anomalous turbulent heat fluxes are primarily driven by changes in SST, rather than the other way around.

Even though Bering Strait OHT is much smaller compared to Atlantic OHT at 65°N, it has an outsized impact on the local sea ice and heat flux variability. Heat fluxes associated with anomalous OHT in the Pacific sector are comparable in magnitude to those in the Atlantic sector. Furthermore, loss of sea ice in the Pacific sector during periods of high Bering Strait OHT generates a substantial heat dome centered on the same area (Fig. 3e). Thus, we emphasize that the local influence of Bering Strait OHT on the atmosphere cannot be neglected.

3.3 Lateral flux decomposition

Next, we compare the effects of Atlantic versus Bering Strait OHT variability on the Arctic atmosphere by decomposing the lateral heat balance. Because the AHT is computed by assuming negligible atmospheric heat storage over decadal timescales, the fluxes may be summed and area-integrated over the Arctic domain to recover the AHT like so:

$$\mathrm{AHT}(\theta) = \int_{\theta}^{\pi/2}\int_{0}^{2\pi} (\mathrm{LW_{sfc}} + \mathrm{SW_{sfc}} + \mathrm{LHF} + \mathrm{SHF}) - (\mathrm{LW_{TOA}} + \mathrm{SW_{TOA}})\, dA$$

where LHF and SHF refer to surface latent heat flux and sensible heat flux, and LW and SW refer to longwave and shortwave radiation respectively. All flux terms above are positive downward to keep consistency with sign conventions in Equation 2. By linearity of integration, we integrate each term separately and refer to each component as an area-integrated flux, denoted as $[F]$:

$$\mathrm{AHT}(\theta) = ([\mathrm{LW_{sfc}}] + [\mathrm{SW_{sfc}}] + [\mathrm{LHF}] + [\mathrm{SHF}]) - ([\mathrm{LW_{TOA}}] + [\mathrm{SW_{TOA}}])$$

We linearly regress each timeseries $[F]$ onto Bering Strait OHT and Atlantic OHT; the linear slopes, with units [TW flux per standard deviation OHT] are shown in Figure 4. A positive slope indicates that positive (resp. negative) OHT anomalies are associated with anomalous flux out of (resp. into) the atmospheric sector through either the surface or TOA, and vice versa for negative slopes.

This decomposition reveals distinct atmospheric responses to OHT through the Atlantic and Bering Strait gateways. Similar to what is found in Figure 2c, there is a stronger compensating AHT anomaly in response to an anomaly in Atlantic OHT than Bering Strait OHT. For both Atlantic and Bering Strait OHT, turbulent heat fluxes are anti-correlated with OHT, consistent with Figure 3c,d. A crucial difference in the atmospheric response can be seen in the TOA longwave radiation. While there is essentially no signal in the Atlantic sector, the Pacific sector experiences strong changes in TOA longwave radiation covarying with anomalous OHT. This longwave flux at the TOA compensates the anomalous turbulent heat fluxes driven by Bering Strait OHT variability. Therefore, the primary mechanism for compensation of OHT anomalies in the Pacific sector is through direct adjustment of the TOA energy balance rather than through changes in AHT.

Furthermore, consistent with the fact that Bering Strait OHT is closely coupled with sea ice in the Pacific sector (Fig. 3a), it is also positively correlated with downwelling shortwave at both the surface and TOA (yellow and orange bars in Fig. 4). This response magnifies the initial ocean-driven heat anomaly via changes in the summertime absorption of shortwave radiation by the ocean.

It remains unclear why atmospheric heat transport does not adjust to compensate significant changes in air-sea heat fluxes in the Pacific sector. Following the mechanism

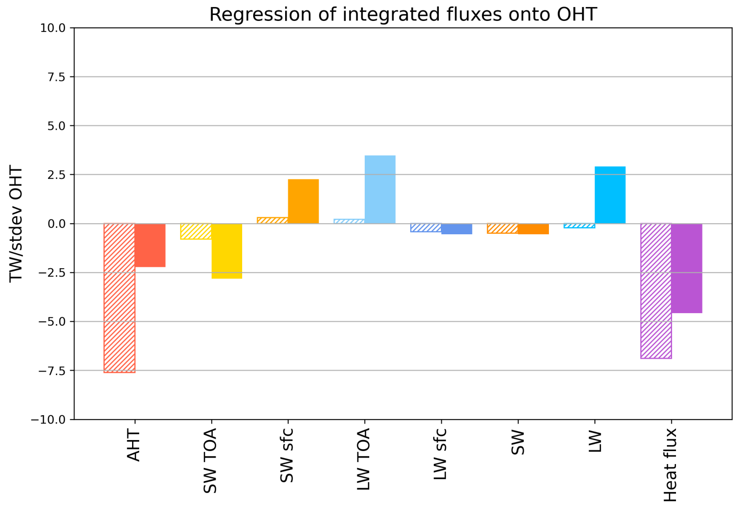

Figure 4. Linear regression slopes of area-integrated flux anomalies onto standardized ocean heat transport. Dashed bars are fluxes regressed onto Atlantic OHT, while solid bars are fluxes regressed onto Bering Strait OHT.

proposed by Swaluw et al. (2007), one would expect air temperature variability over the Pacific sector to affect the local baroclinicity and thereby change the energy transported by atmospheric eddies. One possible reason that this does not translate into compensating AHT is that the mean position of the North Pacific storm track may not extend far enough north for atmospheric eddy heat transport to adjust to changes in baroclinicity centered over the Pacific Arctic. A recent study (Wang et al., 2023) evaluated the Northern Hemisphere storm track in the same simulation used by this study. The mean position of the wintertime storm track (shown in their Figure S1d) indeed extends further north over the Atlantic sector than the Pacific. Therefore, atmospheric eddies may be more efficient at compensating changes in the air-sea heat flux over the Atlantic sector than the Pacific. However, the precise mechanisms that preclude AHT compensation in the Pacific sector are left for future study.

4 Summary and Conclusions

We have shown that decadal variability in Arctic surface air temperature is largely driven by variability of OHT through the Bering Strait in a high-resolution coupled climate simulation. By decomposing the atmospheric response into sector-integrated flux anomalies, we find that Bering Strait OHT anomalies are not damped by Bjerknes Compensation and instead change the TOA longwave energy balance. Thus, Bering Strait OHT, despite its low magnitude compared to Atlantic OHT, has an outsized impact on driving the overall decadal variability in the Arctic.

The main implication of this work is that increases in Bering Strait OHT may be an important driver of future Arctic climate change and, in particular, Arctic Amplification. Our results suggest that even if the total zonally-integrated OHT into the Arctic is compensated by opposing zonally-integrated AHT anomalies—that is, Bjerknes Compensation holds—the comparatively small Bering Strait OHT may still exert significant influence on Arctic climate despite not projecting onto the Bjerknes Compensation signal. In the PI control simulation analyzed here, this is manifested in the decadal variability of sea ice and air temperatures in the Pacific sector.

Our results are consistent with Li et al. (2018), who found that simulated multidecadal variability of September Arctic sea ice extent was impacted to similar degree by both Atlantic OHT and Bering Strait OHT, despite the standard deviation of Bering Strait OHT being an order of magnitude smaller. Furthermore, there is observational evidence that accelerated sea ice loss in the Chukchi Sea is indeed linked to additional northward heat inflow through Bering Strait. Woodgate et al. (2010) found that record high Bering Strait OHT in 2007 contributed to anomalous sea ice loss by triggering earlier onset of seasonal sea ice melt and by providing additional subsurface heat during winter months. Furthermore, in-situ mooring data has revealed an increase in Bering Strait OHT over the past three decades (though data between 1991 to 1999 is missing; Woodgate, 2018). This increase has been attributed, about equally, both to increases in ocean temperatures and northward transport (Woodgate et al., 2012).

We will conclude by noting a few caveats of our work and by proposing some next steps. The robustness of these results depends both on the simulated sea ice climatology and the representation of OHT through the Atlantic and Bering Strait gateways. Therefore, a natural extension of this work is to analyze the relationship between Bering Strait OHT and the Arctic heat budget in other models of both comparable complexity (i.e., high-resolution Earth system models) and lower complexity (e.g., lower resolution models or idealized configurations). Another extension of this work would to consider the mechanisms from a seasonal perspective. Effects of ocean heat transport on sea ice and the overlying atmosphere tend to be amplified in winter, when the ocean is the primary source of heat for the atmosphere while shortwave feedbacks are more prominent in summer (Previdi et al., 2021; Taylor et al., 2022). Finally, to what extent the current analysis of internal climate variability provides lessons for the future of the Arctic also remains to be explored. Chang et al. (in review) demonstrate how improved representation of Bering Strait heat transport in this high-resolution configuration of CESM1.3 increases Arctic warming under a scenario of future anthropogenic forcing compared to a low-resolution configuration of the same model, suggesting that our results have immediate relevance for a future that most likely will feature enhanced OHT through Bering Strait.

5 Open Research

The code used to produce the figures in this study is available upon request to the authors. The model output from the iHESP project is publicly available through the iHESP data archive: `https://ihesp.github.io/archive/products/ds_archive/Sunway_Runs.html`. The CESM1.3-HR simulation is documented in Chang et al. (2020). The NOAA OISST sea ice product is available at `https://www.ncei.noaa.gov/products/optimum-interpolation-sst`.

Acknowledgments

This research was supported by the Regional and Global Model Analysis (RGMA) component of the Earth and Environmental System Modeling (EESM) program of the U.S. Department of Energy's Office of Science, as contribution to the HiLAT-RASM project. Yuchen Li was also supported by the Center for Nonlinear Studies (CNLS) at Los Alamos National Laboratory. We thank Phil Rasch (PNNL) for useful discussions.

References

Bjerknes, J. (1964). Atlantic air-sea interaction. In *Advances in geophysics* (Vol. 10, pp. 1–82). Elsevier.

Chang, P., Zhang, S., Danabasoglu, G., Yeager, S. G., Fu, H., Wang, H., ... Wu, L. (2020). An Unprecedented Set of High-Resolution Earth System Simulations for Understanding Multiscale Interactions in Climate

Variability and Change. *Journal of Advances in Modeling Earth Systems*, *12*(12), e2020MS002298. Retrieved 2023-04-24, from https://onlinelibrary.wiley.com/doi/abs/10.1029/2020MS002298 (_eprint: https://onlinelibrary.wiley.com/doi/pdf/10.1029/2020MS002298) doi: 10.1029/2020MS002298

Chylek, P., Folland, C., Klett, J. D., Wang, M., Hengartner, N., Lesins, G., & Dubey, M. K. (2022). Annual mean arctic amplification 1970–2020: observed and simulated by cmip6 climate models. *Geophysical Research Letters*, *49*(13), e2022GL099371.

Heuzé, C., & Årthun, M. (2019). The Atlantic inflow across the Greenland-Scotland ridge in global climate models (CMIP5). *Elem Sci Anth*, *7*, 16.

Hwang, Y.-T., Frierson, D. M. W., & Kay, J. E. (2011). Coupling between Arctic feedbacks and changes in poleward energy transport. *Geophysical Research Letters*, *38*(17). Retrieved 2022-05-08, from https://onlinelibrary.wiley.com/doi/abs/10.1029/2011GL048546 (_eprint: https://onlinelibrary.wiley.com/doi/pdf/10.1029/2011GL048546) doi: 10.1029/2011GL048546

Jungclaus, J. H., & Koenigk, T. (2010, February). Low-frequency variability of the arctic climate: the role of oceanic and atmospheric heat transport variations. *Climate Dynamics*, *34*(2), 265–279. Retrieved 2022-09-02, from https://doi.org/10.1007/s00382-009-0569-9 doi: 10.1007/s00382-009-0569-9

Kurtakoti, P., Weijer, W., Veneziani, M., Rasch, P. J., & Verma, T. (2023). Sea ice and Cloud Processes Mediating Compensation between Atmospheric and Oceanic Meridional Heat Transports across the CMIP6 Preindustrial Control Experiment. *Journal of Climate*.

Li, D., Zhang, R., & Knutson, T. (2018, February). Comparison of Mechanisms for Low-Frequency Variability of Summer Arctic Sea Ice in Three Coupled Models. *Journal of Climate*, *31*(3), 1205–1226. Retrieved 2023-04-11, from https://journals.ametsoc.org/view/journals/clim/31/3/jcli-d-16-0617.1.xml (Publisher: American Meteorological Society Section: Journal of Climate) doi: 10.1175/JCLI-D-16-0617.1

Liu, Y., Attema, J., & Hazeleger, W. (2020, May). Atmosphere–Ocean Interactions and Their Footprint on Heat Transport Variability in the Northern Hemisphere. *Journal of Climate*, *33*(9), 3691–3710. Retrieved 2022-09-02, from https://journals.ametsoc.org/view/journals/clim/33/9/jcli-d-19-0570.1.xml (Publisher: American Meteorological Society Section: Journal of Climate) doi: 10.1175/JCLI-D-19-0570.1

Liu, Z., Yang, H., He, C., & Zhao, Y. (2016). A theory for Bjerknes compensation: The role of climate feedback. *Journal of Climate*, *29*(1), 191–208.

MacKinnon, J. A., Simmons, H. L., Hargrove, J., Thomson, J., Peacock, T., Alford, M. H., … Wood, K. R. (2021, April). A warm jet in a cold ocean. *Nature Communications*, *12*(1), 2418. Retrieved 2023-07-28, from https://www.nature.com/articles/s41467-021-22505-5 (Number: 1 Publisher: Nature Publishing Group) doi: 10.1038/s41467-021-22505-5

Nummelin, A., Li, C., & Hezel, P. J. (2017). Connecting ocean heat transport changes from the midlatitudes to the Arctic Ocean. *Geophysical Research Letters*, *44*(4), 1899–1908. Retrieved 2022-05-08, from https://onlinelibrary.wiley.com/doi/abs/10.1002/2016GL071333 (_eprint: https://onlinelibrary.wiley.com/doi/pdf/10.1002/2016GL071333) doi: 10.1002/2016GL071333

Outten, S., & Esau, I. (2017, October). Bjerknes compensation in the Bergen Climate Model. *Climate Dynamics*, *49*(7), 2249–2260. Retrieved 2022-01-25, from https://doi.org/10.1007/s00382-016-3447-2 doi: 10.1007/s00382-016-3447-2

Outten, S., Esau, I., & Otterå, O. H. (2018, November). Bjerknes Compensation in the CMIP5 Climate Models. *Journal of Climate*, *31*(21), 8745–8760. Retrieved 2022-01-21, from https://journals.ametsoc.org/doi/10.1175/JCLI-D-18-0058.1 doi: 10.1175/JCLI-D-18-0058.1

Previdi, M., Smith, K. L., & Polvani, L. M. (2021, September). Arctic amplification of climate change: a review of underlying mechanisms. *Environmental Research Letters*, *16*(9), 093003. Retrieved 2022-05-09, from https://iopscience.iop.org/article/10.1088/1748-9326/ac1c29 doi: 10.1088/1748-9326/ac1c29

Rantanen, M., Karpechko, A. Y., Lipponen, A., Nordling, K., Hyvärinen, O., Ruosteenoja, K., … Laaksonen, A. (2022). The arctic has warmed nearly four times faster than the globe since 1979. *Communications Earth & Environment*, *3*(1), 168.

Shaffrey, L., & Sutton, R. (2006, April). Bjerknes Compensation and the Decadal Variability of the Energy Transports in a Coupled Climate Model. *Journal of Climate*, *19*(7), 1167–1181. Retrieved 2022-01-21, from https://journals.ametsoc.org/view/journals/clim/19/7/jcli3652.1.xml (Publisher: American Meteorological Society Section: Journal of Climate) doi: 10.1175/JCLI3652.1

Shu, Q., Wang, Q., Årthun, M., Wang, S., Song, Z., Zhang, M., & Qiao, F. (2022, July). Arctic Ocean Amplification in a warming climate in CMIP6 models. *Science Advances*, *8*(30), eabn9755. Retrieved 2023-09-16, from https://www.science.org/doi/full/10.1126/sciadv.abn9755 (Publisher: American Association for the Advancement of Science) doi: 10.1126/sciadv.abn9755

Swaluw, E. v. d., Drijfhout, S. S., & Hazeleger, W. (2007, December). Bjerknes Compensation at High Northern Latitudes: The Ocean Forcing the Atmosphere. *Journal of Climate*, *20*(24), 6023–6032. Retrieved 2022-01-21, from https://journals.ametsoc.org/view/journals/clim/20/24/2007jcli1562.1.xml (Publisher: American Meteorological Society Section: Journal of Climate) doi: 10.1175/2007JCLI1562.1

Taylor, P. C., Boeke, R. C., Boisvert, L. N., Feldl, N., Henry, M., Huang, Y., … others (2022). Process drivers, inter-model spread, and the path forward: A review of amplified Arctic warming. *Frontiers in Earth Science*, *9*, 758361.

Tsubouchi, T., Våge, K., Hansen, B., Larsen, K. M. H., Østerhus, S., Johnson, C., … Valdimarsson, H. (2021, January). Increased ocean heat transport into the Nordic Seas and Arctic Ocean over the period 1993–2016. *Nature Climate Change*, *11*(1), 21–26. Retrieved 2023-09-15, from https://www.nature.com/articles/s41558-020-00941-3 (Number: 1 Publisher: Nature Publishing Group) doi: 10.1038/s41558-020-00941-3

Wang, Z., Li, M., Zhang, S., Small, R. J., Lu, L., Yuan, M., … Wu, L. (2023). The Northern Hemisphere Wintertime Storm Track Simulated in the High-Resolution Community Earth System Model. *Journal of Advances in Modeling Earth Systems*, *15*(10), e2023MS003652. Retrieved 2023-11-08, from https://onlinelibrary.wiley.com/doi/abs/10.1029/2023MS003652 (_eprint: https://onlinelibrary.wiley.com/doi/pdf/10.1029/2023MS003652) doi: 10.1029/2023MS003652

Woodgate, R. A. (2018, January). Increases in the Pacific inflow to the Arctic from 1990 to 2015, and insights into seasonal trends and driving mechanisms from year-round Bering Strait mooring data. *Progress in Oceanography*, *160*, 124–154. Retrieved 2023-07-27, from https://www.sciencedirect.com/science/article/pii/S0079661117302215 doi: 10.1016/j.pocean.2017.12.007

Woodgate, R. A., Weingartner, T., & Lindsay, R. (2010). The 2007 Bering Strait oceanic heat flux and anomalous Arctic sea-ice retreat. *Geophysical Research Letters*, *37*(1). Retrieved 2023-07-27, from https://onlinelibrary.wiley.com/doi/abs/10.1029/2009GL041621 (_eprint: https://onlinelibrary.wiley.com/doi/pdf/10.1029/2009GL041621) doi: 10.1029/2009GL041621

Woodgate, R. A., Weingartner, T. J., & Lindsay, R. (2012). Observed increases in Bering Strait oceanic fluxes from the Pacific to the Arctic from 2001 to 2011 and their impacts on the Arctic Ocean water column. *Geophysical Research Letters*, *39*(24). Retrieved 2023-07-27, from `https://onlinelibrary.wiley.com/doi/abs/10.1029/2012GL054092` (_eprint: https://onlinelibrary.wiley.com/doi/pdf/10.1029/2012GL054092) doi: 10.1029/2012GL054092

Zhang, R. (2015). Mechanisms for low-frequency variability of summer arctic sea ice extent. *Proceedings of the National Academy of Sciences*, *112*(15), 4570–4575. Retrieved from `https://www.pnas.org/doi/10.1073/pnas.1422296112` doi: 10.1073/pnas.1422296112

Bering Strait Ocean Heat Transport Drives Decadal Arctic Variability in a High-Resolution Climate Model

Yuchen Li[1,2*], Wilbert Weijer[2,3], Prajvala Kurtakoti[4,2], Milena Veneziani[2], Ping Chang[5]

[1]Stanford University, Stanford, CA, USA
[2]Los Alamos National Laboratory, Los Alamos, NM, USA
[3]International Arctic Research Center, University of Alaska Fairbanks, Fairbanks, AK, USA
[4]Johns Hopkins University, Baltimore, MD, USA
[5]Texas A&M University, College Station, TX, USA

Key Points:

- Ocean heat transport variability through the Bering Strait has an outsized effect on Arctic sea ice cover and surface temperature
- Atlantic ocean heat transport anomalies into the Arctic are compensated by atmospheric heat transport anomalies on decadal timescales

*450 Jane Stanford Way Stanford, CA 94305–2004

Corresponding author: Yuchen Li, `yucli@stanford.edu`

Abstract

We investigate the role of ocean heat transport (OHT) in driving the decadal variability of the Arctic climate by analyzing the pre-industrial control simulation of a high-resolution climate model. While the OHT variability at 65°N is greater in the Atlantic, we find that the decadal variability of Arctic-wide surface temperature and sea ice area is much better correlated with Bering Strait OHT than Atlantic OHT. In particular, decadal Bering Strait OHT variability causes significant changes in local sea ice cover and air-sea heat fluxes, which are amplified by shortwave feedbacks. These heat flux anomalies are regionally balanced by longwave radiation at the top of the atmosphere, without compensation by atmospheric heat transport (Bjerknes compensation). The sensitivity of the Arctic to changes in OHT may thus rely on an accurate representation of the heat transport through the Bering Strait, which is difficult to resolve in coarse-resolution ocean models.

Plain Language Summary

We studied how ocean heat transport (OHT) affects decade-timescale variability in the Arctic climate using a high-resolution climate model. Specifically, we compared the impacts of heat entering the Arctic Ocean through the Nordic Seas from the Atlantic and through the Bering Strait from the Pacific. Though more heat is transported from the Atlantic, Arctic surface temperature and sea ice respond more strongly to changes in OHT through the Bering Strait. Unlike Atlantic OHT, changes in Bering Strait OHT impact local air temperatures directly, without compensating changes in atmospheric heat transport. Proper representation of the Arctic's sensitivity to future increased OHT may thus rely on correctly representing OHT through Bering Strait, which is challenging in coarse-resolution ocean models.

1 Introduction

The Arctic is warming faster than the rest of the world (Rantanen et al., 2022; Chylek et al., 2022). This amplification of Arctic climate change is caused by a coupling between local feedbacks and increased poleward heat transport from lower latitudes (Hwang et al., 2011; Nummelin et al., 2017; Previdi et al., 2021). However, the mechanisms of this coupling are complex and still poorly understood.

Decadal to multidecadal timescale variability in the Arctic—manifested by changes in sea ice extent, surface temperatures, etc.—has been previously shown to be closely related to ocean heat transport (Zhang, 2015; Jungclaus & Koenigk, 2010). Further, it has been suggested that variability in *total* heat transport into the Arctic is reduced by a phenomenon known as Bjerknes Compensation (BC), whereby anomalies in meridional ocean heat transport (OHT) tend to induce roughly equal and opposite anomalies in meridional atmospheric heat transport (AHT). Bjerknes (1964) proposed that this result follows from energy conservation on timescales where the top-of-atmosphere (TOA) fluxes and ocean heat content remain approximately constant. A recent study (Y. Liu et al., 2020) indeed found evidence of decadal-timescale BC in several reanalysis datasets and confirmed the importance of surface heat fluxes in communicating OHT variability to the atmosphere. However, as they note, the exact causal relationships of decadal-timescale heat transport variability are very difficult to parse out in such short observational time series.

Models have thus been indispensable to the study of BC due to the need for sufficiently long time series. In coupled global climate models, BC is typically strongest at the high northern latitudes (Shaffrey & Sutton, 2006; Swaluw et al., 2007; Outten & Esau, 2017; Jungclaus & Koenigk, 2010), due to the presence of strong regional climate feedbacks in the marginal ice zone (Z. Liu et al., 2016; Kurtakoti et al., 2023). Specifically, Swaluw et al. (2007) and Outten and Esau (2017) argue that BC in high northern latitudes is due to the modulation of sea ice by decadal Atlantic OHT variability. The canonical mechanism is illustrated as follows: positive OHT anomalies melt back sea ice, enhancing heat loss from the previously ice-covered ocean. The anomalous heat flux into the atmosphere may be amplified by local radiative feedbacks such as the ice-albedo feedback, causing local atmospheric warming. This warming then reduces the meridional temperature gradient and thus baroclinity, reducing the northward heat transport by atmospheric eddies.

This canonical perspective does not take into account significant longitudinal variations in the Earth's geography and climate mean state. In particular, OHT from the sub-Arctic to the Arctic Ocean takes place primarily through two main gateways: flow across the Greenland-Scotland Ridge connects the Arctic Ocean to the subpolar North Atlantic Ocean, while flow through the Bering Strait connects the Arctic to the subpolar North Pacific. OHT through the Atlantic sector is an order of magnitude larger than that through the Bering Strait, both in mean value and in amplitude of variability. Consequently, most studies on the connection between decadal Arctic variability and Bjerknes Compensation have focused mainly on Atlantic OHT variability. An exception is the study by Li et al. (2018), who analyzed three Earth system models (ESM) and demonstrated that OHT through both gateways has an important impact on Arctic climate. In fact, they argue that OHT through Bering Strait is more efficient in causing low-frequency variability of Arctic sea ice than OHT through the Atlantic sector. A strong sensitivity of Arctic sea ice on Bering Strait throughflow has also been found in observations (Woodgate et al., 2012; MacKinnon et al., 2021).

This raises the question: how does the atmosphere respond to OHT variability through the different gateways given the differences in sea ice sensitivity, and what are the consequences for the atmosphere's ability to compensate for this OHT variability?

This question is important for several reasons. First, observations over the past few decades (Woodgate, 2018; Tsubouchi et al., 2021) as well as model projections of future climate change (Shu et al., 2022) show a robust increase of northward OHT going into the Arctic from both the subpolar North Atlantic and North Pacific Oceans. The extent to which AHT will compensate these changes is therefore of primary concern for constraining uncertainty in Arctic climate change. Second, the current generation of climate models typically have a spatial resolution of $\sim 1°$ in their standard configuration ocean models. Such low resolution leaves narrow channels like the Bering Strait significantly underresolved (Chang et al., in review), while poorly resolved bathymetry also appears to weaken OHT across the Greenland-Scotland Ridge (Heuzé & Årthun, 2019). Consequently, OHT in standard resolution climate models may be significantly biased, and their results should be treated with caution.

Recently, an unprecedented multi-century simulation of a high-resolution global climate model was performed (Chang et al., 2020), which at the time of analysis was the longest pre-industrial control simulation run at high resolution (see Data and Methods). In this paper we use this unique data set to investigate the Arctic atmospheric response to OHT variability through the primary oceanic gateways. We find that Bering Strait OHT plays an outsized role in driving Arctic climate variability. By decomposing the meridional energy balance, we show that while the AHT partially compensates for anomalies in the zonally-integrated OHT, lateral atmospheric energy fluxes do not compensate for anomalies in OHT through Bering Strait.

2 Data and Methods

We use a portion of the 500-year pre-industrial (PI) control simulation of CESM1.3 (Community Earth System Model version 1.3), configured with nominal horizonal res-

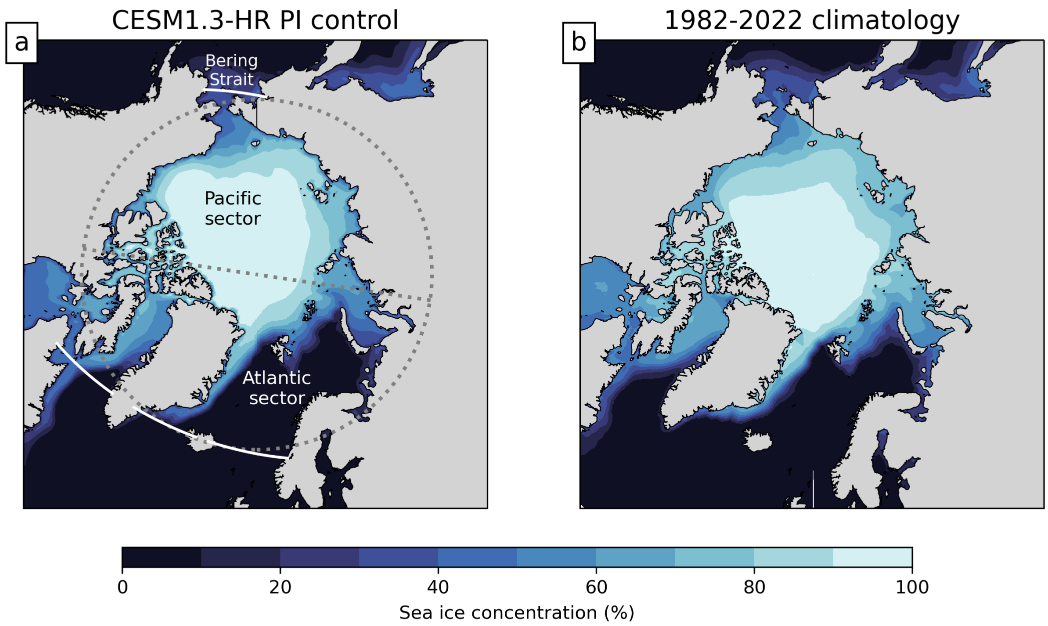

Figure 1. (a) Annual-mean climatology of Arctic sea ice concentration in the PI control simulation analyzed in this study. The dotted grey lines show 65°N and the boundary between the Pacific and Atlantic sectors defined in this paper. The white lines indicate the logical latitudes used for integration. (b) Observed 1982-2022 climatology of annual-mean Arctic sea ice concentration (NOAA OISST v2).

olutions of 0.25°in the atmosphere and land models and 0.1°in the ocean and sea-ice models (Chang et al., 2020). The PI control was forced with greenhouse gas conditions kept constant at the 1850 levels throughout the simulation. We exclude the first 150 years from our analysis due to model drift, so all time series are 350 years long (see Chang et al., 2020, for context). The sea ice climatology of the PI control simulation is shown in Figure 1a and shows good agreement with the observed climatology during the satellite era (Fig. 1b).

We estimate meridional OHT and AHT at 65°N from monthly-averaged fields. We choose 65°N as the boundary of the Arctic, however our results are not sensitive to the choice of latitude. The OHT time series is calculated by integrating the product of meridional velocity (v) and potential temperature (Θ):

$$\mathrm{OHT} = \int_{\varphi_E}^{\varphi_W} \int_{-H}^{0} c_p v \Theta \cos\theta \, \mathrm{d}z \; R_e \mathrm{d}\varphi \tag{1}$$

where we use θ and φ to denote latitude and longitude, respectively. φ_E and φ_W denote the eastern and western boundaries of the basin and H, c_p, z, and R_e denote basin depth, heat capacity of seawater at constant pressure, vertical depth, and the radius of the Earth, respectively. This reconstruction, which ignores contributions by sub-monthly covariance between velocity and temperature, is necessary because the model's online diagnostic OHT output was corrupted for the first 277 years and thus would have significantly shortened the available timespan for our analysis. For ease of computation, we also choose to approximate OHT across 65°N by heat transport across a *logical* latitude line of the model's tripolar grid that tracks 65°N reasonably well. A comparison between our OHT time series, the OHT time series from the model's online diagnostic output across the same logical latitude line (after the period of data corruption), and an estimate of the OHT across the actual 65°N latitude line, shows that our OHT time series is an accurate representation of OHT across 65°N in the Atlantic (Supplementary Information).

The AHT time series is estimated by assuming a negligible atmospheric heat capacity and cumulatively integrating the energy flux divergence (e.g., Shaffrey & Sutton, 2006; Swaluw et al., 2007; Outten et al., 2018). We define AHT at the north pole ($\theta = \pi/2$) to be zero and integrate the zonally-integrated flux divergence southward to find the AHT at each latitude θ:

$$\text{AHT} = \int_{\theta}^{\pi/2} \int_{0}^{2\pi} (F_{\text{sfc}} - F_{\text{TOA}}) R_e^2 \cos\theta' \, \mathrm{d}\varphi \, \mathrm{d}\theta' \tag{2}$$

where F_{TOA} and F_{sfc} are the net downward heat flux at the top-of-atmosphere and surface, respectively. By this formulation, northward AHT is positive.

Since we are concerned with variability on decadal timescales, all monthly time series are annually-averaged, detrended, and then smoothed using a 10-year moving average. Moreover, to account for inflated Pearson's r when regressing smoothed time series, we calculate an effective number of degrees of freedom for significance tests. We follow the formulation given in Jungclaus and Koenigk (2010) to estimate the effective number of samples:

$$n_{\text{eff}} = \frac{n}{1 + 2(\sum_{i=1}^{n} r_i r_i')} \tag{3}$$

where n is the original length of the time series and r_i, r_i' are the autocorrelations of the two time series at lag i. For smoothed time series originally with 341 samples, n_{eff} is on the order of 30-50.

3 Results

3.1 Arctic response to Pacific and Atlantic OHT

The OHT through the Atlantic and Bering Strait (the blue and red lines in Figure 2, respectively) both display decadal to multidecadal variability. OHT anomalies are positively correlated with Arctic-average surface air temperature anomalies and negatively correlated with sea ice area anomalies (Figure 2a,b). Strikingly, Bering Strait OHT (mean = 8.6 TW, standard deviation = 1.4 TW) has a stronger correlation with both surface temperature and sea ice than Atlantic OHT (mean = 342 TW, standard deviation = 10.5 TW), even though it is considerably smaller in magnitude. It is not possible to conclude from correlation alone whether 1) OHT variability is driving these changes in temperature and sea ice, 2) OHT variability is driven by surface temperature changes, or 3) OHT, temperature, and sea ice covary due to another driving mode of variability. In later sections, however, we present evidence indicating that OHT plays the driving role in modulating sea ice and air-sea heat flux, thus communicating ocean heat anomalies to the atmosphere.

At 65°N, anomalies in AHT and Atlantic OHT compensate each other on decadal timescales, with an anticorrelation of $r = -0.61$ (Figure 2c). The compensation is inconsistent over time, with some periods displaying almost perfect compensation, while others show undercompensation (where the magnitude of the AHT anomaly is less than the magnitude of the OHT anomaly) or overcompensation (where the magnitude of the AHT anomaly exceeds the magnitude of the OHT anomaly). Moreover, Bering Strait OHT is not correlated with the AHT. In general, the *total* OHT (not shown here) and AHT anomalies are opposite in sign, indicative of Bjerknes compensation on a decadal timescale.

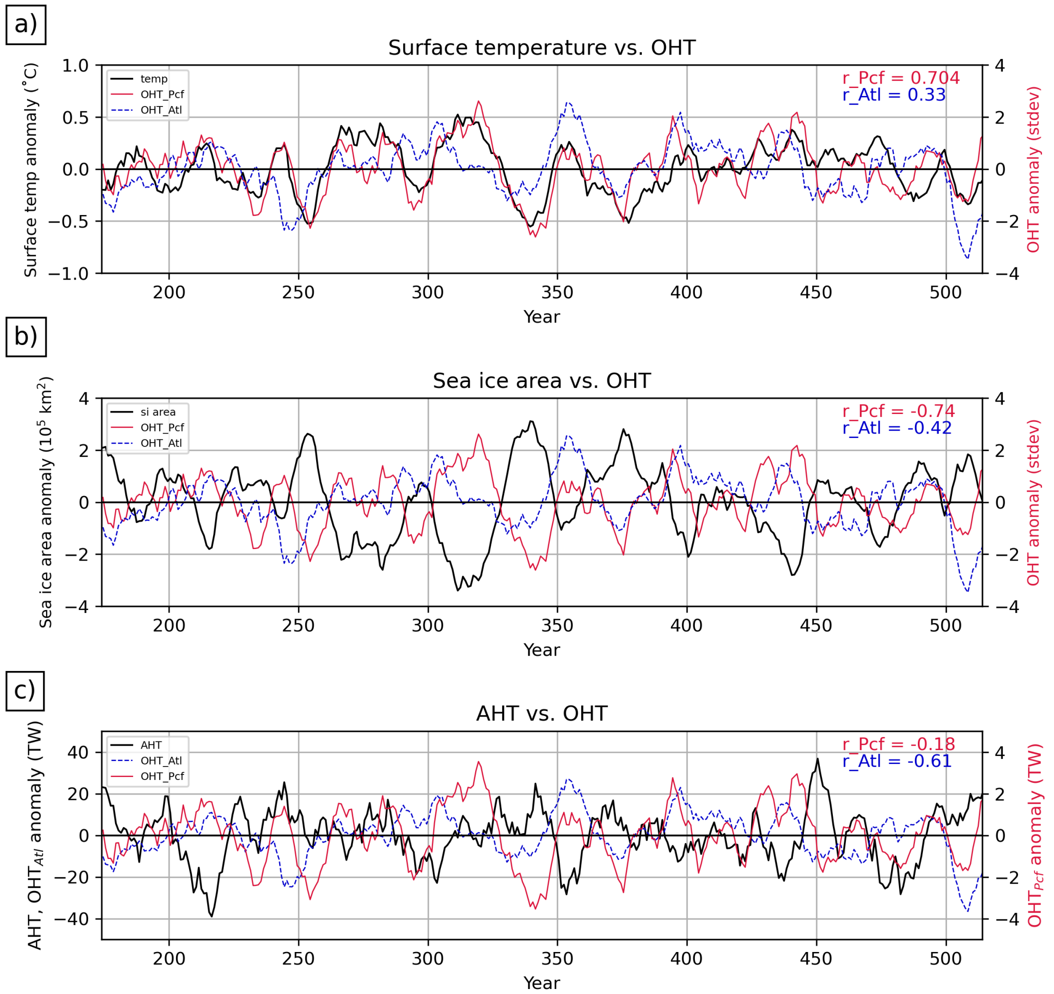

Figure 2. **(a)**: Area-averaged surface air temperature anomaly over the Arctic domain (black) plotted with standardized Bering Strait (red) and Atlantic (blue, dotted) OHT anomalies. **(b)**: same as (a), but sea ice area anomaly (black) is shown instead of temperature. **(c)**: same as (a), but AHT anomaly (black) is shown instead of temperature. The time series are not standardized to emphasize their magnitudes. Note that in (c) the vertical scale for Bering Strait OHT has been magnified by a factor of 10 for better visibility. Pearson's r correlation coefficients are given in the top right.

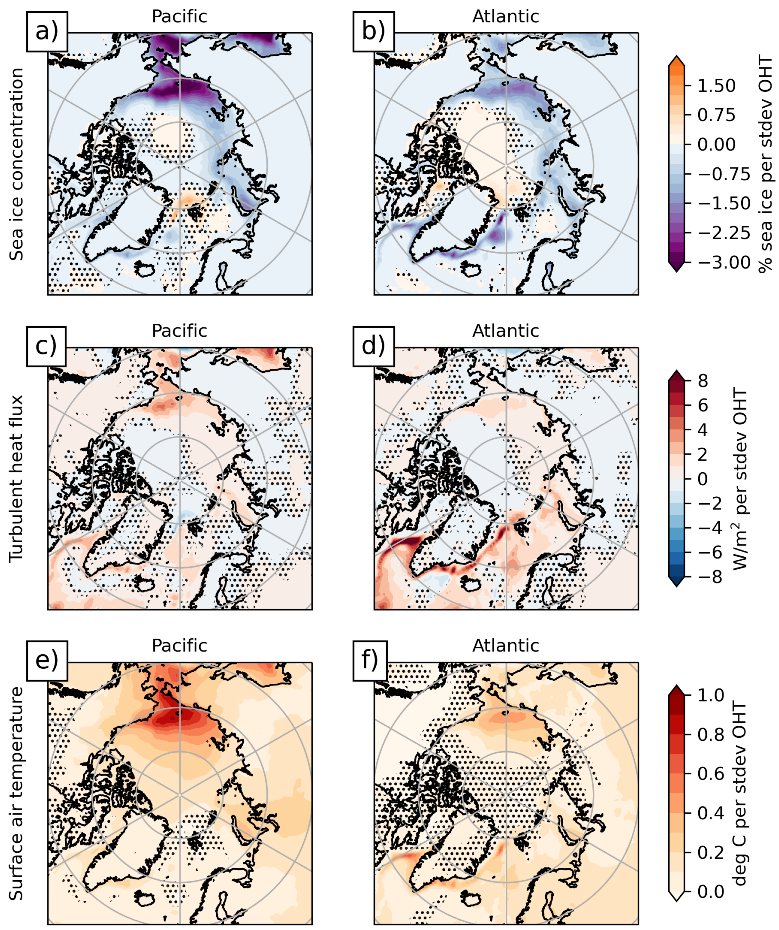

Figure 3. **(a)**: regression of 10-year moving mean sea ice concentration anomalies onto the standardized Bering Strait OHT anomalies at 65°N. Stippling indicates statistical insignificance with respect to a $p = 0.05$ threshold. **(b)**: as in (a), but regressed onto Atlantic OHT. **(c)**: as in (a), but turbulent heat fluxes (defined as sensible plus latent surface heat flux with positive going from ocean to atmosphere). **(d)**: as in (c), but regressed onto Atlantic OHT. **(e):** as in (a), but surface air temperature. **(f):** as in (e), but regressed onto Atlantic OHT.

3.2 Bering Strait OHT Drives Variability in the Pacific Sector

To better understand the atmosphere-ocean interaction that mediates these distinct OHT-AHT relationships, we regress the sea ice anomaly, surface turbulent heat flux (defined as the sum of latent and sensible heat fluxes) anomaly, and surface air temperature anomaly onto the standardized OHT anomaly across 65°N.

Figure 3 shows the linear regressions of anomalous sea ice concentration, turbulent heat flux, and surface temperature onto the OHT anomaly through Bering Strait and the Atlantic separately. During periods of anomalously high OHT, ice is lost in the marginal ice zone and anomalous heat flux is transferred from the newly exposed ocean to the atmosphere. The greatest changes associated with Atlantic OHT variability occur along the East Greenland Current while the greatest changes associated with Bering Strait OHT variability occur in the Chukchi Sea. The greatest changes in surface heat flux are found at the marginal ice zone, similar to what was found in Outten and Esau (2017), Jungclaus and Koenigk (2010), and Kurtakoti et al. (2023). Regression of anomalous sea surface temperatures (SST) onto OHT reveals a spatial pattern similar to the heat flux regression (Figure S1). This positive correlation between SST and heat flux indicates that anomalous turbulent heat fluxes are primarily driven by changes in SST, rather than the other way around.

Even though Bering Strait OHT is much smaller compared to Atlantic OHT at 65°N, it has an outsized impact on the local sea ice and heat flux variability. Heat fluxes associated with anomalous OHT in the Pacific sector are comparable in magnitude to those in the Atlantic sector. Furthermore, loss of sea ice in the Pacific sector during periods of high Bering Strait OHT generates a substantial heat dome centered on the same area (Fig. 3e). Thus, we emphasize that the local influence of Bering Strait OHT on the atmosphere cannot be neglected.

3.3 Lateral flux decomposition

Next, we compare the effects of Atlantic versus Bering Strait OHT variability on the Arctic atmosphere by decomposing the lateral heat balance. Because the AHT is computed by assuming negligible atmospheric heat storage over decadal timescales, the fluxes may be summed and area-integrated over the Arctic domain to recover the AHT like so:

$$\mathrm{AHT}(\theta) = \int_{\theta}^{\pi/2} \int_{0}^{2\pi} (\mathrm{LW_{sfc}} + \mathrm{SW_{sfc}} + \mathrm{LHF} + \mathrm{SHF}) - (\mathrm{LW_{TOA}} + \mathrm{SW_{TOA}}) \, dA$$

where LHF and SHF refer to surface latent heat flux and sensible heat flux, and LW and SW refer to longwave and shortwave radiation respectively. All flux terms above are positive downward to keep consistency with sign conventions in Equation 2. By linearity of integration, we integrate each term separately and refer to each component as an area-integrated flux, denoted as $[F]$:

$$\mathrm{AHT}(\theta) = ([\mathrm{LW_{sfc}}] + [\mathrm{SW_{sfc}}] + [\mathrm{LHF}] + [\mathrm{SHF}]) - ([\mathrm{LW_{TOA}}] + [\mathrm{SW_{TOA}}])$$

We linearly regress each timeseries $[F]$ onto Bering Strait OHT and Atlantic OHT; the linear slopes, with units [TW flux per standard deviation OHT] are shown in Figure 4. A positive slope indicates that positive (resp. negative) OHT anomalies are associated with anomalous flux out of (resp. into) the atmospheric sector through either the surface or TOA, and vice versa for negative slopes.

This decomposition reveals distinct atmospheric responses to OHT through the Atlantic and Bering Strait gateways. Similar to what is found in Figure 2c, there is a stronger compensating AHT anomaly in response to an anomaly in Atlantic OHT than Bering Strait OHT. For both Atlantic and Bering Strait OHT, turbulent heat fluxes are anti-correlated with OHT, consistent with Figure 3c,d. A crucial difference in the atmospheric response can be seen in the TOA longwave radiation. While there is essentially no signal in the Atlantic sector, the Pacific sector experiences strong changes in TOA longwave radiation covarying with anomalous OHT. This longwave flux at the TOA compensates the anomalous turbulent heat fluxes driven by Bering Strait OHT variability. Therefore, the primary mechanism for compensation of OHT anomalies in the Pacific sector is through direct adjustment of the TOA energy balance rather than through changes in AHT.

Furthermore, consistent with the fact that Bering Strait OHT is closely coupled with sea ice in the Pacific sector (Fig. 3a), it is also positively correlated with downwelling shortwave at both the surface and TOA (yellow and orange bars in Fig. 4). This response magnifies the initial ocean-driven heat anomaly via changes in the summertime absorption of shortwave radiation by the ocean.

It remains unclear why atmospheric heat transport does not adjust to compensate significant changes in air-sea heat fluxes in the Pacific sector. Following the mechanism

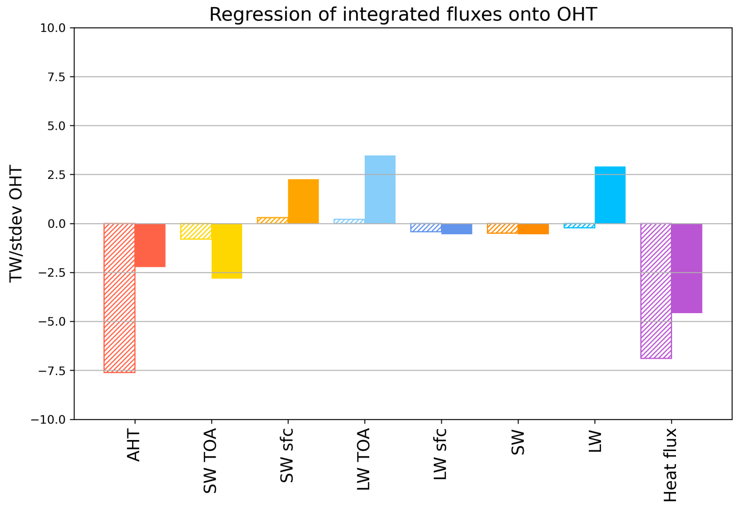

Figure 4. Linear regression slopes of area-integrated flux anomalies onto standardized ocean heat transport. Dashed bars are fluxes regressed onto Atlantic OHT, while solid bars are fluxes regressed onto Bering Strait OHT.

proposed by Swaluw et al. (2007), one would expect air temperature variability over the Pacific sector to affect the local baroclinicity and thereby change the energy transported by atmospheric eddies. One possible reason that this does not translate into compensating AHT is that the mean position of the North Pacific storm track may not extend far enough north for atmospheric eddy heat transport to adjust to changes in baroclinicity centered over the Pacific Arctic. A recent study (Wang et al., 2023) evaluated the Northern Hemisphere storm track in the same simulation used by this study. The mean position of the wintertime storm track (shown in their Figure S1d) indeed extends further north over the Atlantic sector than the Pacific. Therefore, atmospheric eddies may be more efficient at compensating changes in the air-sea heat flux over the Atlantic sector than the Pacific. However, the precise mechanisms that preclude AHT compensation in the Pacific sector are left for future study.

4 Summary and Conclusions

We have shown that decadal variability in Arctic surface air temperature is largely driven by variability of OHT through the Bering Strait in a high-resolution coupled climate simulation. By decomposing the atmospheric response into sector-integrated flux anomalies, we find that Bering Strait OHT anomalies are not damped by Bjerknes Compensation and instead change the TOA longwave energy balance. Thus, Bering Strait OHT, despite its low magnitude compared to Atlantic OHT, has an outsized impact on driving the overall decadal variability in the Arctic.

The main implication of this work is that increases in Bering Strait OHT may be an important driver of future Arctic climate change and, in particular, Arctic Amplification. Our results suggest that even if the total zonally-integrated OHT into the Arctic is compensated by opposing zonally-integrated AHT anomalies—that is, Bjerknes Compensation holds—the comparatively small Bering Strait OHT may still exert significant influence on Arctic climate despite not projecting onto the Bjerknes Compensation signal. In the PI control simulation analyzed here, this is manifested in the decadal variability of sea ice and air temperatures in the Pacific sector.

Our results are consistent with Li et al. (2018), who found that simulated multidecadal variability of September Arctic sea ice extent was impacted to similar degree by both Atlantic OHT and Bering Strait OHT, despite the standard deviation of Bering Strait OHT being an order of magnitude smaller. Furthermore, there is observational evidence that accelerated sea ice loss in the Chukchi Sea is indeed linked to additional northward heat inflow through Bering Strait. Woodgate et al. (2010) found that record high Bering Strait OHT in 2007 contributed to anomalous sea ice loss by triggering earlier onset of seasonal sea ice melt and by providing additional subsurface heat during winter months. Furthermore, in-situ mooring data has revealed an increase in Bering Strait OHT over the past three decades (though data between 1991 to 1999 is missing; Woodgate, 2018). This increase has been attributed, about equally, both to increases in ocean temperatures and northward transport (Woodgate et al., 2012).

We will conclude by noting a few caveats of our work and by proposing some next steps. The robustness of these results depends both on the simulated sea ice climatology and the representation of OHT through the Atlantic and Bering Strait gateways. Therefore, a natural extension of this work is to analyze the relationship between Bering Strait OHT and the Arctic heat budget in other models of both comparable complexity (i.e., high-resolution Earth system models) and lower complexity (e.g., lower resolution models or idealized configurations). Another extension of this work would to consider the mechanisms from a seasonal perspective. Effects of ocean heat transport on sea ice and the overlying atmosphere tend to be amplified in winter, when the ocean is the primary source of heat for the atmosphere while shortwave feedbacks are more prominent in summer (Previdi et al., 2021; Taylor et al., 2022). Finally, to what extent the current analysis of internal climate variability provides lessons for the future of the Arctic also remains to be explored. Chang et al. (in review) demonstrate how improved representation of Bering Strait heat transport in this high-resolution configuration of CESM1.3 increases Arctic warming under a scenario of future anthropogenic forcing compared to a low-resolution configuration of the same model, suggesting that our results have immediate relevance for a future that most likely will feature enhanced OHT through Bering Strait.

5 Open Research

The code used to produce the figures in this study is available upon request to the authors. The model output from the iHESP project is publicly available through the iHESP data archive: `https://ihesp.github.io/archive/products/ds_archive/Sunway_Runs.html`. The CESM1.3-HR simulation is documented in Chang et al. (2020). The NOAA OISST sea ice product is available at `https://www.ncei.noaa.gov/products/optimum-interpolation-sst`.

Acknowledgments

This research was supported by the Regional and Global Model Analysis (RGMA) component of the Earth and Environmental System Modeling (EESM) program of the U.S. Department of Energy's Office of Science, as contribution to the HiLAT-RASM project. Yuchen Li was also supported by the Center for Nonlinear Studies (CNLS) at Los Alamos National Laboratory. We thank Phil Rasch (PNNL) for useful discussions.

References

Bjerknes, J. (1964). Atlantic air-sea interaction. In *Advances in geophysics* (Vol. 10, pp. 1–82). Elsevier.

Chang, P., Zhang, S., Danabasoglu, G., Yeager, S. G., Fu, H., Wang, H., ... Wu, L. (2020). An Unprecedented Set of High-Resolution Earth System Simulations for Understanding Multiscale Interactions in Climate

Variability and Change. *Journal of Advances in Modeling Earth Systems*, *12*(12), e2020MS002298. Retrieved 2023-04-24, from https://onlinelibrary.wiley.com/doi/abs/10.1029/2020MS002298 (_eprint: https://onlinelibrary.wiley.com/doi/pdf/10.1029/2020MS002298) doi: 10.1029/2020MS002298

Chylek, P., Folland, C., Klett, J. D., Wang, M., Hengartner, N., Lesins, G., & Dubey, M. K. (2022). Annual mean arctic amplification 1970–2020: observed and simulated by cmip6 climate models. *Geophysical Research Letters*, *49*(13), e2022GL099371.

Heuzé, C., & Årthun, M. (2019). The Atlantic inflow across the Greenland-Scotland ridge in global climate models (CMIP5). *Elem Sci Anth*, *7*, 16.

Hwang, Y.-T., Frierson, D. M. W., & Kay, J. E. (2011). Coupling between Arctic feedbacks and changes in poleward energy transport. *Geophysical Research Letters*, *38*(17). Retrieved 2022-05-08, from https://onlinelibrary.wiley.com/doi/abs/10.1029/2011GL048546 (_eprint: https://onlinelibrary.wiley.com/doi/pdf/10.1029/2011GL048546) doi: 10.1029/2011GL048546

Jungclaus, J. H., & Koenigk, T. (2010, February). Low-frequency variability of the arctic climate: the role of oceanic and atmospheric heat transport variations. *Climate Dynamics*, *34*(2), 265–279. Retrieved 2022-09-02, from https://doi.org/10.1007/s00382-009-0569-9 doi: 10.1007/s00382-009-0569-9

Kurtakoti, P., Weijer, W., Veneziani, M., Rasch, P. J., & Verma, T. (2023). Sea ice and Cloud Processes Mediating Compensation between Atmospheric and Oceanic Meridional Heat Transports across the CMIP6 Preindustrial Control Experiment. *Journal of Climate*.

Li, D., Zhang, R., & Knutson, T. (2018, February). Comparison of Mechanisms for Low-Frequency Variability of Summer Arctic Sea Ice in Three Coupled Models. *Journal of Climate*, *31*(3), 1205–1226. Retrieved 2023-04-11, from https://journals.ametsoc.org/view/journals/clim/31/3/jcli-d-16-0617.1.xml (Publisher: American Meteorological Society Section: Journal of Climate) doi: 10.1175/JCLI-D-16-0617.1

Liu, Y., Attema, J., & Hazeleger, W. (2020, May). Atmosphere–Ocean Interactions and Their Footprint on Heat Transport Variability in the Northern Hemisphere. *Journal of Climate*, *33*(9), 3691–3710. Retrieved 2022-09-02, from https://journals.ametsoc.org/view/journals/clim/33/9/jcli-d-19-0570.1.xml (Publisher: American Meteorological Society Section: Journal of Climate) doi: 10.1175/JCLI-D-19-0570.1

Liu, Z., Yang, H., He, C., & Zhao, Y. (2016). A theory for Bjerknes compensation: The role of climate feedback. *Journal of Climate*, *29*(1), 191–208.

MacKinnon, J. A., Simmons, H. L., Hargrove, J., Thomson, J., Peacock, T., Alford, M. H., ... Wood, K. R. (2021, April). A warm jet in a cold ocean. *Nature Communications*, *12*(1), 2418. Retrieved 2023-07-28, from https://www.nature.com/articles/s41467-021-22505-5 (Number: 1 Publisher: Nature Publishing Group) doi: 10.1038/s41467-021-22505-5

Nummelin, A., Li, C., & Hezel, P. J. (2017). Connecting ocean heat transport changes from the midlatitudes to the Arctic Ocean. *Geophysical Research Letters*, *44*(4), 1899–1908. Retrieved 2022-05-08, from https://onlinelibrary.wiley.com/doi/abs/10.1002/2016GL071333 (_eprint: https://onlinelibrary.wiley.com/doi/pdf/10.1002/2016GL071333) doi: 10.1002/2016GL071333

Outten, S., & Esau, I. (2017, October). Bjerknes compensation in the Bergen Climate Model. *Climate Dynamics*, *49*(7), 2249–2260. Retrieved 2022-01-25, from https://doi.org/10.1007/s00382-016-3447-2 doi: 10.1007/s00382-016-3447-2

Outten, S., Esau, I., & Otterå, O. H. (2018, November). Bjerknes Compensation in the CMIP5 Climate Models. *Journal of Climate*, *31*(21), 8745–8760. Retrieved 2022-01-21, from `https://journals.ametsoc.org/doi/10.1175/JCLI-D-18-0058.1` doi: 10.1175/JCLI-D-18-0058.1

Previdi, M., Smith, K. L., & Polvani, L. M. (2021, September). Arctic amplification of climate change: a review of underlying mechanisms. *Environmental Research Letters*, *16*(9), 093003. Retrieved 2022-05-09, from `https://iopscience.iop.org/article/10.1088/1748-9326/ac1c29` doi: 10.1088/1748-9326/ac1c29

Rantanen, M., Karpechko, A. Y., Lipponen, A., Nordling, K., Hyvärinen, O., Ruosteenoja, K., ... Laaksonen, A. (2022). The arctic has warmed nearly four times faster than the globe since 1979. *Communications Earth & Environment*, *3*(1), 168.

Shaffrey, L., & Sutton, R. (2006, April). Bjerknes Compensation and the Decadal Variability of the Energy Transports in a Coupled Climate Model. *Journal of Climate*, *19*(7), 1167–1181. Retrieved 2022-01-21, from `https://journals.ametsoc.org/view/journals/clim/19/7/jcli3652.1.xml` (Publisher: American Meteorological Society Section: Journal of Climate) doi: 10.1175/JCLI3652.1

Shu, Q., Wang, Q., Årthun, M., Wang, S., Song, Z., Zhang, M., & Qiao, F. (2022, July). Arctic Ocean Amplification in a warming climate in CMIP6 models. *Science Advances*, *8*(30), eabn9755. Retrieved 2023-09-16, from `https://www.science.org/doi/full/10.1126/sciadv.abn9755` (Publisher: American Association for the Advancement of Science) doi: 10.1126/sciadv.abn9755

Swaluw, E. v. d., Drijfhout, S. S., & Hazeleger, W. (2007, December). Bjerknes Compensation at High Northern Latitudes: The Ocean Forcing the Atmosphere. *Journal of Climate*, *20*(24), 6023–6032. Retrieved 2022-01-21, from `https://journals.ametsoc.org/view/journals/clim/20/24/2007jcli1562.1.xml` (Publisher: American Meteorological Society Section: Journal of Climate) doi: 10.1175/2007JCLI1562.1

Taylor, P. C., Boeke, R. C., Boisvert, L. N., Feldl, N., Henry, M., Huang, Y., ... others (2022). Process drivers, inter-model spread, and the path forward: A review of amplified Arctic warming. *Frontiers in Earth Science*, *9*, 758361.

Tsubouchi, T., Våge, K., Hansen, B., Larsen, K. M. H., Østerhus, S., Johnson, C., ... Valdimarsson, H. (2021, January). Increased ocean heat transport into the Nordic Seas and Arctic Ocean over the period 1993–2016. *Nature Climate Change*, *11*(1), 21–26. Retrieved 2023-09-15, from `https://www.nature.com/articles/s41558-020-00941-3` (Number: 1 Publisher: Nature Publishing Group) doi: 10.1038/s41558-020-00941-3

Wang, Z., Li, M., Zhang, S., Small, R. J., Lu, L., Yuan, M., ... Wu, L. (2023). The Northern Hemisphere Wintertime Storm Track Simulated in the High-Resolution Community Earth System Model. *Journal of Advances in Modeling Earth Systems*, *15*(10), e2023MS003652. Retrieved 2023-11-08, from `https://onlinelibrary.wiley.com/doi/abs/10.1029/2023MS003652` (_eprint: https://onlinelibrary.wiley.com/doi/pdf/10.1029/2023MS003652) doi: 10.1029/2023MS003652

Woodgate, R. A. (2018, January). Increases in the Pacific inflow to the Arctic from 1990 to 2015, and insights into seasonal trends and driving mechanisms from year-round Bering Strait mooring data. *Progress in Oceanography*, *160*, 124–154. Retrieved 2023-07-27, from `https://www.sciencedirect.com/science/article/pii/S0079661117302215` doi: 10.1016/j.pocean.2017.12.007

Woodgate, R. A., Weingartner, T., & Lindsay, R. (2010). The 2007 Bering Strait oceanic heat flux and anomalous Arctic sea-ice retreat. *Geophysical Research Letters*, *37*(1). Retrieved 2023-07-27, from `https://onlinelibrary.wiley.com/doi/abs/10.1029/2009GL041621` (_eprint: https://onlinelibrary.wiley.com/doi/pdf/10.1029/2009GL041621) doi: 10.1029/2009GL041621

Woodgate, R. A., Weingartner, T. J., & Lindsay, R. (2012). Observed increases in Bering Strait oceanic fluxes from the Pacific to the Arctic from 2001 to 2011 and their impacts on the Arctic Ocean water column. *Geophysical Research Letters*, *39*(24). Retrieved 2023-07-27, from https://onlinelibrary.wiley.com/doi/abs/10.1029/2012GL054092 (_eprint: https://onlinelibrary.wiley.com/doi/pdf/10.1029/2012GL054092) doi: 10.1029/2012GL054092

Zhang, R. (2015). Mechanisms for low-frequency variability of summer arctic sea ice extent. *Proceedings of the National Academy of Sciences*, *112*(15), 4570–4575. Retrieved from https://www.pnas.org/doi/10.1073/pnas.1422296112 doi: 10.1073/pnas.1422296112

Supporting Information for "Bering Strait Ocean Heat Transport Drives Decadal Arctic Variability in a High-Resolution Climate Model"

Yuchen Li[1,2 *], Wilbert Weijer[2,3], Prajvala Kurtakoti[2], Milena Veneziani[2],

Ping Chang[4]

[1]Stanford University, Stanford, CA, USA

[2]Los Alamos National Laboratory, Los Alamos, NM, USA

[3]International Arctic Research Center, University of Alaska Fairbanks, Fairbanks, AK, USA

[4]Texas A&M University, College Station, TX, USA

Contents of this file

---

[*]450 Jane Stanford Way Stanford, CA

94305–2004

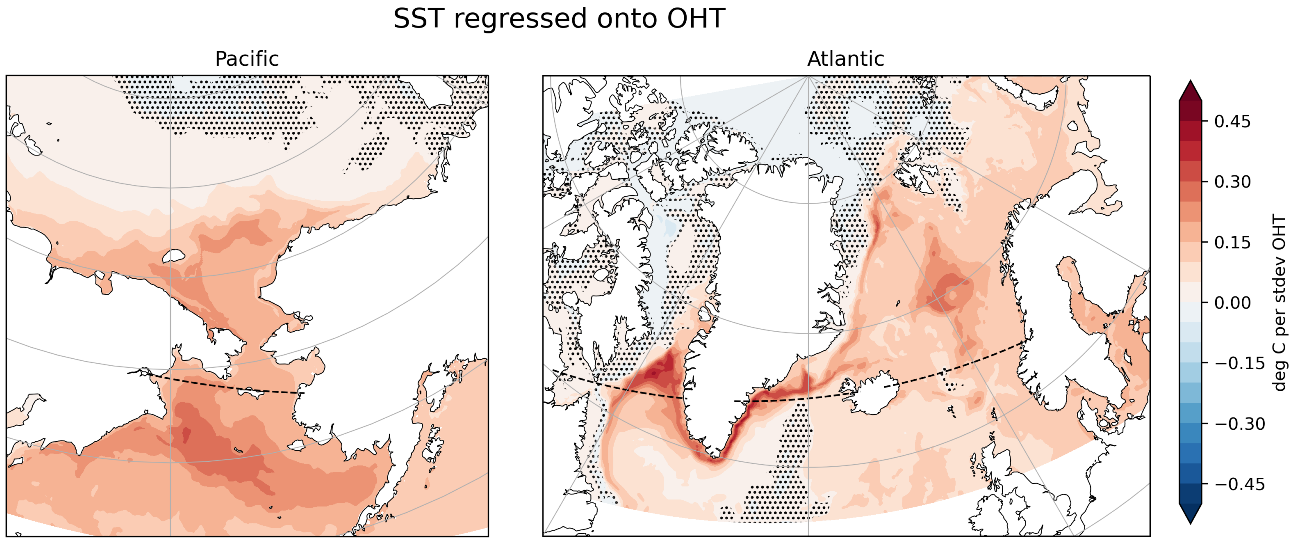

Figure S1. Sea surface temperature anomaly regressed onto standardized Bering Strait (Left) and Atlantic (Right) OHT anomaly. Regressions are between timeseries smoothed with a 10-year moving mean to emphasize decadal timescale relationships. Stippling indicates statistical insignificance above the $p = 0.05$ threshold. The pseudo-zonal dashed lines indicate the oceanic gateways for which OHT is calculated